A physiologically-based pharmacokinetic model for predicting doxorubicin disposition in multiple tissue levels and quantitative toxicity assessment

Fang-Ching Chao, Eloísa Berbel Manaia, Gilles Ponchel, Chien-Ming Hsieh

Biomedicine & Pharmacotherapy 168 (2023) 115636

Contents lists available at ScienceDirect

Biomedicine & Pharmacotherapy

journal homepage: www.elsevier.com/locate/biopha

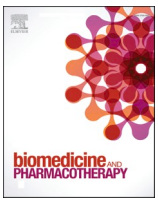

A physiologically-based pharmacokinetic model for predicting doxorubicin disposition in multiple tissue levels and quantitative toxicity assessment

Fang-Ching Chao [a], Eloísa Berbel Manaia [a], Gilles Ponchel [a,*], Chien-Ming Hsieh [b,c,**]

[a] CNRS UMR 8612, Institut Galien Paris-Saclay, Université Paris-Saclay, Orsay 91400, France
[b] School of Pharmacy, College of Pharmacy, Taipei Medical University, Taipei 11031, Taiwan
[c] Ph.D. Program in Drug Discovery and Development Industry, College of Pharmacy, Taipei Medical University, Taipei 11031, Taiwan

ARTICLE INFO

Keywords:
Physiologically-based pharmacokinetics
Doxorubicin
Interspecies extrapolation
Disposition
Quantitative pharmacology
Toxicity

ABSTRACT

Doxorubicin is a widely-used chemotherapeutic drug, however its high toxicity poses a significant challenge for its clinical use. To address this issue, a physiologically-based pharmacokinetic (PBPK) model was implemented to quantitatively assess doxorubicin toxicity at cellular scale. Due to its unique pharmacokinetic behavior (e.g. high volume of distribution and affinity to extra-plasma tissue compartments), we proposed a modified PBPK model structure and developed the model with multispecies extrapolation to compensate for the limitation of obtaining clinical tissue data. Our model predicted the disposition of doxorubicin in multiple tissues including clinical tissue data with an overall absolute average fold error (AAFE) of 2.12. The model's performance was further validated with 8 clinical datasets in combined with intracellular doxorubicin concentration with an average AAFE of 1.98. To assess the potential cellular toxicity, toxicity levels and area under curve (AUC) were defined for different dosing regimens in toxic and non-toxic scenarios. The cellular concentrations of doxorubicin in multiple organ sites associated with commonly observed adverse effects (AEs) were simulated and calculated the AUC for quantitative assessments. Our findings supported the clinical dosing regimen of 75 mg/m^2 with a 21-day interval and suggest that slow infusion and separated single high doses may lower the risk of developing AEs from a cellular level, providing valuable insights for the risk assessment of doxorubicin chemotherapy. In conclusion, our work highlights the potential of PBPK modelling to provide quantitative assessments of cellular toxicity and supports the use of clinical dosing regimens to mitigate the risk of adverse effects.

1. Introduction

Doxorubicin is a multi-action chemotherapeutic agent indicated to several types of cancer (e.g. acute lymphoblastic and myeloblastic leukemia, (non-)Hodgkin lymphoma, and several metastatic carcinomas) [1]. Despite the fact that its high therapeutic efficacy against multiple cancers, doxorubicin also possesses dozens of adverse effects (AEs). The affected organs range from dermatological, gastrointestinal, and hematological to cardiovascular and so on. The most concerning aspect of treating patients with doxorubicin is the cardiovascular-associated AEs, such as ECG changes, cardiotoxicity, and arrhythmia. These AEs may result in treatment discontinuation, and a maximum lifetime cumulative dose of 550 mg/m^2 is recommended to reduce the risk of developing cardiomyopathy. Since then, Doxil®, a liposomal form of doxorubicin [2] was introduced and has demonstrated a favourable toxicity profile compared to the free drug [3], but its use is also limited. Despite this, no research has provided a quantitative assessment or guidance based on clinical data from a tissue or cellular perspective, apart from the recommended maximum lifetime cumulative dose.

Doxorubicin's pharmacokinetic (PK) behavior is characterized by a rapid distribution half-life of approximately 5 min and a terminal half-life ranging from 20 to 48 h, along with a high volume of distribution between 809 and 1214 L/m^2 in human [1]. A significant proportion of doxorubicin (approximately 75%) binds to plasma proteins, and its elimination is primarily mediated via metabolism (50%), biliary excretion (40%), and renal excretion (10%) [4,5]. These distinct PK profiles are likely attributed to doxorubicin's pronounced affinity for the extra-plasmatic tissue compartment [6]. Therefore, an accurate and

* Correspondence to: CNRS UMR 8612, Institut Galien Paris-Saclay, Université Paris-Saclay, 17 avenue des Sciences, Orsay 91400, France.
** Correspondence to: School of Pharmacy, College of Pharmacy, Taipei Medical University & D. Program in Drug Discovery and Development Industry, College of Pharmacy, Taipei Medical University, 250 Wu-Hsing Street, Taipei City 11031, Taiwan.
E-mail addresses: gilles.ponchel@universite-paris-saclay.fr (G. Ponchel), cmhsieh@tmu.edu.tw (C.-M. Hsieh).

https://doi.org/10.1016/j.biopha.2023.115636
Received 20 July 2023; Received in revised form 22 September 2023; Accepted 3 October 2023
Available online 10 October 2023

Table 1
The publication information for clinically observed data obtained from various dosing schedules.

Publication	Dosing schedule	n	Collected sample	Reference
Erttmann et al. (1988)	15 mg/m^2 i.v. q10h 4 doses	8	Plasma	[22]
Bugat et al. (1989)	15 mg/m^2/day i.v. for 3 days	4–17	Plasma	[23]
Muller et al. (1993)	36 mg/m^2 i.v.	5	Plasma and blood mononuclear cell	[24]
Muller et al. (1993)	9 mg/m^2/day i.v. for 3 days	5	Plasma and blood mononuclear cell	[24]
Speth et al. (1987a)	30 mg/m^2 i.v.	9	Plasma and bone marrow leukocyte[a]	[25]
Speth et al. (1987a)	9 mg/m^2/day i.v. for 3 days	7	Plasma and bone marrow leukocyte[a]	[25]
Speth et al. (1987b)	30 mg/m^2 i.v. q4d 3 doses	1	Plasma and bone marrow leukocyte[a]	[26]
Speth et al. (1987b)	30 mg/m^2/day i.v. for 3 days	2	Plasma and bone marrow leukocyte[a]	[26]
Speth et al. (1987b)	30 mg/m^2/8 h i.v. qd 3 doses	4	Plasma and bone marrow leukocyte[a]	[26]
Speth et al. (1987b)	30 mg/m^2 i.v. qd 3 doses	7	Plasma and bone marrow leukocyte[a]	[26]

Table 2
Estimated parameters for PBPK model.

Parameter	Definition	Value (CV%)	Unit	Estimation Method
P_{para}	Permeability coefficient of Dox transport through endothelial pores	0.02 (14.34)	cm/min	Computationally
$SF_{rbc/pls}$	Scaling factor for partitional coefficient of red blood cells	10	-	Manually
$SF_{int/pls}$,	Scaling factor for partitional coefficient of interstitial space	595.84 (9.05)	-	Computationally
$SF_{cell/pls}$	Scaling factor for partitional coefficient of all cellular components except red blood cells	133.04 (36.17)	-	Computationally
K_{bile}	Bile elimination rate of Dox	610.91 (72.80)	1/hour	Computationally
$SF_{Metabolism}$	Scaling factor for saturable enzymatic metabolism	2.79 (58.15)	-	Computationally

comprehensive understanding of doxorubicin's in vivo distribution across different tissues is crucial and should not be solely based on plasma drug concentrations, which may pose limitations in sample collection.

Physiologically-based pharmacokinetic (PBPK) modelling has been demonstrated to have a strong predictive power for drug disposition and simulating clinical outcomes. The model incorporates the realistic physical and anatomical structures of various tissues using a mechanistic approach, along with species-specific physiological and drug-related parameters, as recommended by health authorities [7,8]. PBPK model has also been widely used for inter-species, route, and drug extrapolation in both preclinical and clinical settings [9,10]. Furthermore, the model has found applications in toxicology for estimating chemical risks, accounting for interindividual variability [11,12]. By integrating preclinical or clinical data, the model can be calibrated and verified to accurately simulate drug disposition in the virtual human body. However, the model's complexity, involving multiple compartments and parameters, and the limited availability of clinical tissue samples often restrict the clinical application of PBPK modelling to plasma concentration measurements. This approach can lead to concerns of overparameterization and overfitting, necessitating a cautious approach when applying PBPK modelling in clinical practice [12–14].

The aim of the study was to propose an improved PBPK model structure that would incorporate physical and anatomical structures with constrained parameters, thereby addressing concerns of overfitting. In addition, we utilized an interspecies extrapolation approach to calibrate and verify the model, given the challenge of obtaining clinical tissue data. The study's focus was on validating the metabolism and elimination behavior of doxorubicin to ensure the model accurately reflected the drug's PK behavior. Additionally, to leverage the full potential of the PBPK model, we investigated drug concentration at a cellular level and compared our results to clinical data. We determined the potential cellular concentration that could cause cytotoxicity and defined corresponding toxicity levels, which we used to evaluate the toxicity of multiple clinical and reported dosing regimens both qualitatively and quantitatively.

This doxorubicin PBPK model has generated novel insights on clinical doxorubicin treatment risk management, providing a quantitative approach on a cellular scale. Our findings demonstrate the importance of using a PBPK model with a realistic structure and constrained parameters, along with an interspecies extrapolation approach, to improve PK predictions and better inform clinical decision-making.

2. Methods

To predict drug concentrations in different organs and sub-organs, we constructed, calibrated, and validated our PBPK model using a three-steps approach. Firstly, we developed and verified the model structure through interspecies extrapolation from mouse to rat, rabbit, dog, and human, concerning not only plasma concentrations but also organ concentrations, which have limited human data.

Secondly, we confirmed the calibrated model using a different set of clinically observed data and multiple dosing schedules to ensure accurate predictions of both plasma and cellular concentrations. Lastly, we used the fully validated model to simulate reported doxorubicin toxicity dosing, and lifetime cumulative doses, providing a quantitative assessment of doxorubicin toxicity at a cellular level.

2.1. PBPK model development

A whole-body PBPK model was constructed in MATLAB 2022a (MathWorks, Natick, MA), that incorporates optimization, analysis, and plotting functionalities. Standard animal weights of 20 g, 300 g, 3 kg, 12 kg, and 70 kg (with a body surface area: 1.75 m^2) for the mouse, rat, rabbit, dog, and human, respectively, were utilized to construct the model. The PBPK model structure took the open source PBPK software platform PK-Sim® [15,16] as basis and integrated features such as leukocyte compartment from recently reported model structures [17–19]. Additionally, we incorporated compartments and equations that accurately describe the elimination and metabolism of doxorubicin through urine, bile, and metabolism, enabling realistic representation of drug elimination and metabolism behavior. The published datasets from different species used for model verification were demonstrated in Supplementary Material 1 Section 1. Supplementary Material 2 contains detailed information on the model's differential equations, structure,

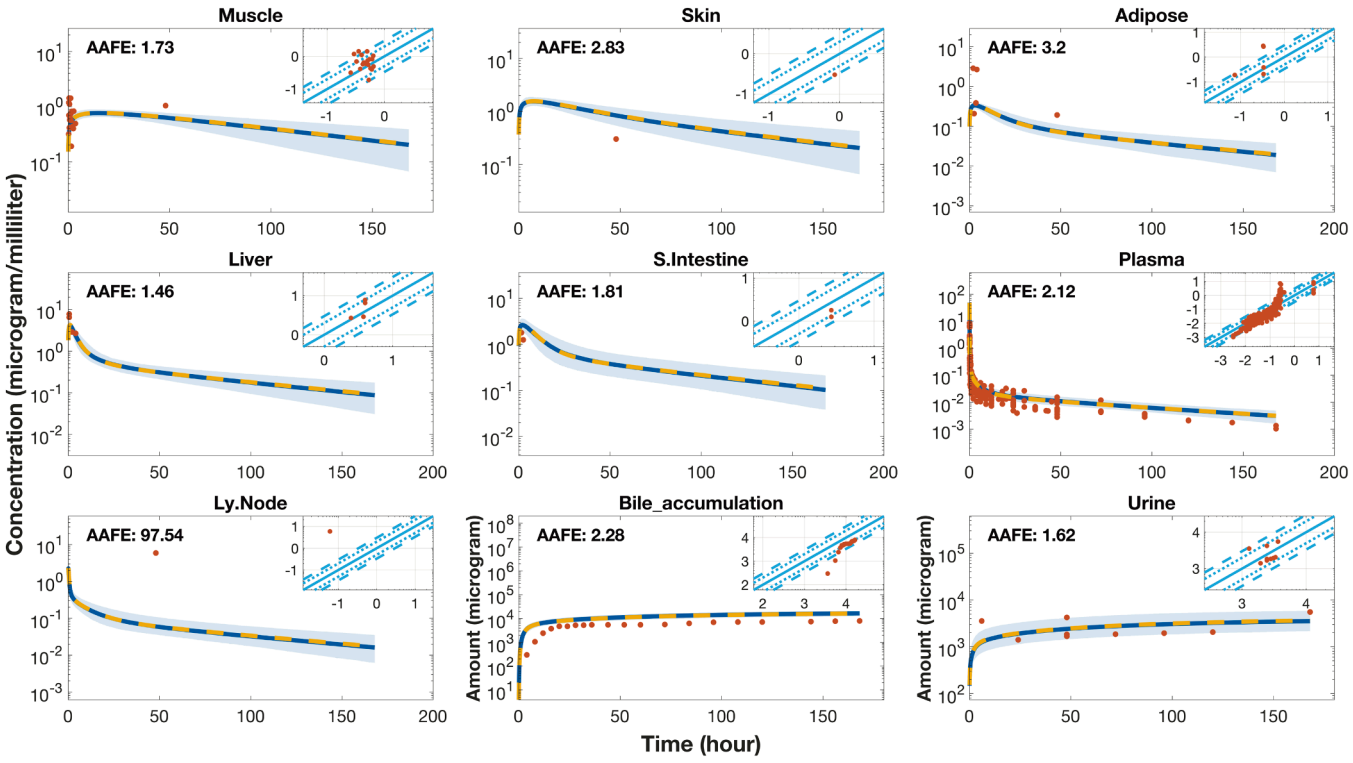

Fig. 1. The comparison of predicted and observed pharmacokinetic (PK) data for doxorubicin in human across various organs. The concentration-time profile of the observed data is depicted in orange dots superimposed onto simulation results, represented by a yellow dashed line indicating the best-fitted curve. The median, 5th, and 95th percentiles from the Monte Carlo simulation are shown by a blue line and shaded area. Additionally, the average absolute fold error (AAFE) is calculated for each organ. Each organ subplot includes a plot comparing predicted and observed doxorubicin concentrations at corresponding time points. Orange dots represent the predicted concentration values, while a diagonal blue line, dot line, and dashed line indicate the perfect fit, 2-fold error range, and 3-fold error range, respectively.

parameters, and other pertinent details.

To account for individual variability, Monte Carlo simulation was implemented, and details are available in Supplementary Material 1 Section 2. The PBPK model was initially calibrated in mice and subsequently extrapolated to human by integrating species-specific physiological parameters, thereby enabling us to evaluate model prediction performance in multiple organs. The metabolism and elimination of doxorubicin was assessed to verify that the model accurately captured the drug's in vivo disposition. Additionally, the local and global sensitivity analysis were performed to better understand the influence of optimized parameters on multiple model outputs, as described in Supplementary Material 1 Sections 3 and 4. The evaluations of the model's prediction performance was qualitatively conducted by plotting the concentration-time profile of the predicted and the observed data along with predicted versus observed data were compared with a 2 and 3-fold error range. The absolute average fold error (AAFE; Equation1) was calculated as a quantitative evaluation.

$$AAFE = 10^{\frac{\sum|\log\frac{pred}{obs}|}{N}} \quad (1)$$

where pred and obs are prediction and observation data; N is the total number of observations.

Considering the individual variability and uncertainty across multiple publications and several organs, AAFE under 3 was considered acceptable prediction performance.

2.2. Model verification against clinically observed data from different dosing schedules

The calibrated doxorubicin PBPK model from multispecies extrapolation was further verified by five clinical publications with 10 datasets that employed different dosing schedules. These publications provided concentration-time profiles for both plasma and cellular concentration (Table 1). The concentration-time profiles were digitized using WebPlotDigitizer V.4.4 (https://automeris.io/WebPlotDigitizer). Plasma data was collected, while data for blood mononuclear cells and bone marrow leukocytes were collected based on the data availability. To calculate cellular concentration, we assumed a leukocyte size of around 100 fL and considered 10^{10} cells as 1 mL [20]. Blood plasma and blood plasma leukocyte simulations were carried out to compare plasma and blood mononuclear cell data, respectively. For bone marrow leukocyte data, both bone plasma leukocyte and bone interstitial leukocyte were simulated in the context of the bone marrow sample collection method [21]. The model prediction performance was qualitatively evaluated by plotting the concentration-time profile of the predicted and the observed data and quantitatively evaluated by calculating the AAFE as previous mention. Considering the realistic and biologically reasonable of the data and the simulations, the cellular drug concentration was also evaluated with defined doxorubicin cellular toxicity levels (detailed in Supplementary Material 1 Section 5) from level 1–5 have a doxorubicin concentration of 0.01, 0.07, 0.27, 1.09, and 18.9 μg/mL.

To perform a quantitative assessment of the effects of doxorubicin, a two-step approach was followed. First, a commonly used single-agent dosing regimen of 75 mg/m^2 with a 21 days interval was simulated on both organ and sub-organ scales. The impact of metabolism and elimination was also incorporated into the evaluation. Cellular toxicity levels were defined to obtain an overview of doxorubicin concentration on different scales. Secondly, heart cellular and stomach cellular drug concentrations were simulated to evaluate the associated adverse effects (AEs) on the cardiovascular and gastrointestinal systems. Hematologic adverse effects were evaluated by simulating blood plasma leukocyte, bone cellular, bone plasma leukocyte, and interstitial leukocyte drug

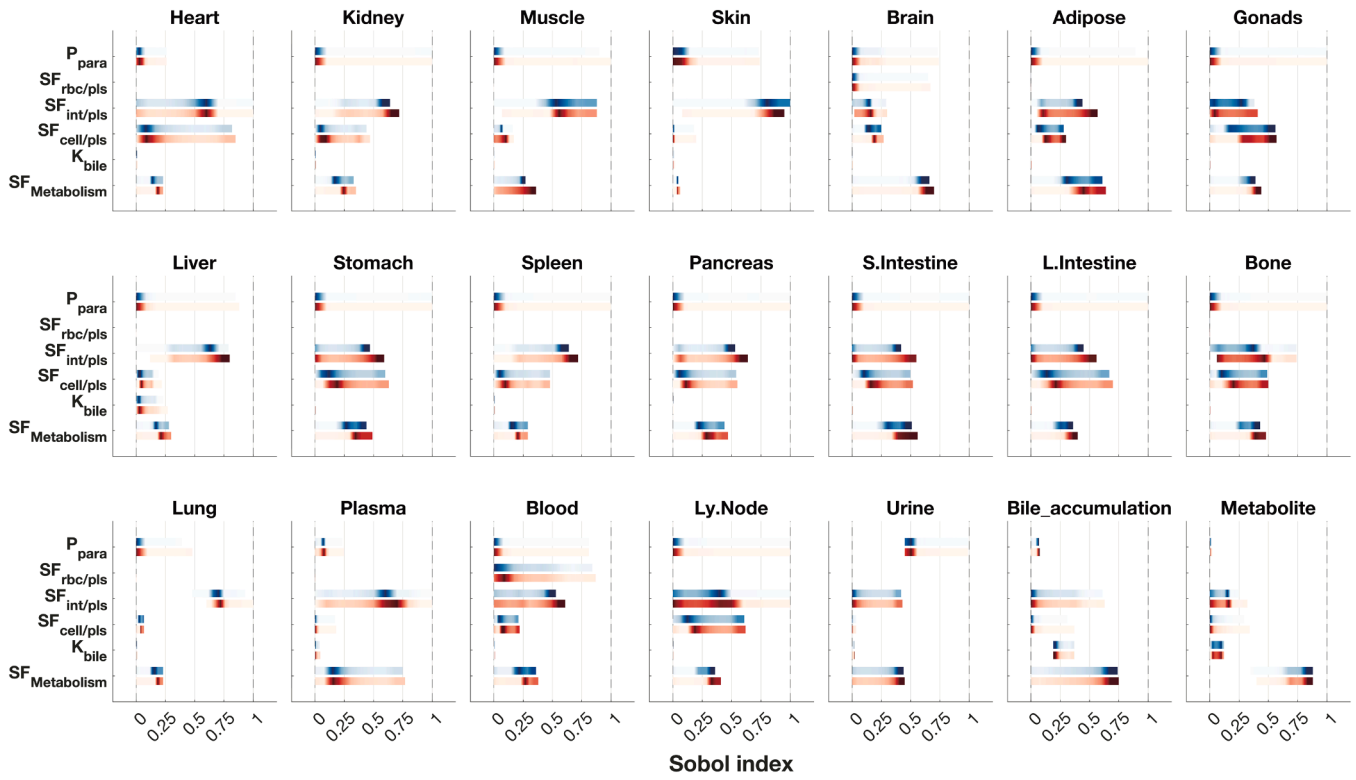

Fig. 2. The global sensitivity analysis was performed using estimated parameters as model inputs and concentration-time profiles for all 17 organs, blood plasma, and the metabolism and elimination compartments were used as model outputs. The first and total order Sobol indices were calculated and presented as blue and red horizontal bars, respectively. Sensitivities that occurred frequently throughout the entire time course were presented with darker colors. The abbreviation used are: S. Intestine (small intestine) L.Intestine (large intestine) Ly.Node (lymph node), Bile_accumulation (accumulated bile eliminated doxorubicin).

concentrations. Similarly, skin and adipose cellular drug concentrations were simulated to assess dermatological adverse effects. Blood plasma drug concentration was used for reference purposes.

Dosing regimen were simulated for various scenarios, including two reported accidental overdose cases of doxorubicin [27], with dosing regimens of 540 mg i.v. with 0.75 h infusion and 150 mg i.v. qd 2 doses. A single dose of 150 mg/m^2 i.v., which is considered as fatal dose [5] according to Micromedex® Drug Reference, was simulated for toxicity assessment. For non-toxic assessment, commonly used clinical dosing regimens [1] of 75 mg/m^2, 30 mg/m^2 i.v. qd 3 doses, and 100 mg/m^2 i.v. 72 h infusion were simulated. Additionally, the lifetime cumulative dose of 550 mg/m^2 was compared using a dosing regimen of 75 mg/m^2 i.v. q3w 8 doses to a dosing regimen of 20 mg/m^2 i.v. qw 30 doses, which Weiss & Manthel (1977) [28] claimed patients could tolerate at higher lifetime cumulative dose.

The area under the curve (AUC) was calculated using defined doxorubicin cellular toxicity levels for the simulated sub-compartments drug concentration to obtain a quantitative assessment.

We also utilized defined cellular toxicity levels along with the simulated drug concentration in sub-compartments to obtain a quantitative assessment. This assessment involved calculating the area under the curve (AUC) exceeding the defined cellular toxicity levels 0.01, 0.07, 0.27, 1.09, and 18.9 μg/mL, denoted as AUC_{L1}, AUC_{L2}, AUC_{L3}, AUC_{L4}, and AUC_{L5}, respectively, with a unit of μg/mL*h.

3. Results

3.1. Model construction and simulations

To prevent overfitting, six main parameters, including P_{para}, $SF_{rbc/pls}$, $SF_{int/pls}$, $SF_{cell/pls}$, K_{bile}, and $SF_{Metabolism}$ were manually or computationally estimated. With these parameters, the doxorubicin disposition across mouse, rat, rabbit, dog, and human was successfully described, and the optimized value for each parameter was determined with acceptable precision as shown in Table 2. The $SF_{rbc/pls}$ was manually fitted due to low sensitivity to model outputs. The K_{bile} and $SF_{Metabolism}$ perfectly captured the elimination and metabolism behavior of doxorubicin. After 168 hrs, the metabolite accumulation, bile excretion, and renal elimination amounted to 62%, 30%, and 6% of the initial dose, respectively, which is consistent with the clinical data reported.

The simulation results showed that the model was able to describe the doxorubicin concentration in multiple organs and also concerning the realism of the metabolism and elimination compared to the observed data (human data was shown in Fig. 1, and other species data were shown in Supplementary Material 1 Figs. S2–5). Furthermore, the majority of the data points were within the 90th percentile of the Monte Carlo simulation. The prediction versus observation plot showed that the most of the data points had an error range of 2–3-fold. Quantitatively, most organs had an AAFE below 2.5, resulting in an overall AAFE of 2.12 across all human data.

The global sensitivity analysis (Fig. 2) for the estimated parameters indicated that the $SF_{int/pls}$, $SF_{cell/pls}$, and $SF_{Metabolism}$ had the greatest influence on the model outputs. Conversely, K_{bile} exhibited a considerable impact solely on drug concentration in the liver, as well as accumulated bile elimination (Bile_accumulation), and accumulated metabolite. Meanwhile, P_{para} and $K_{rbc/pls}$ only had a minor impact on general model outputs. Comparison of the total-order to the first-order Sobol index for all the outputs suggested that there were minor interactions among these parameters.

3.2. Model verification against clinically observed data from different dosing schedules

The model exhibited a high degree of accuracy in predicting plasma

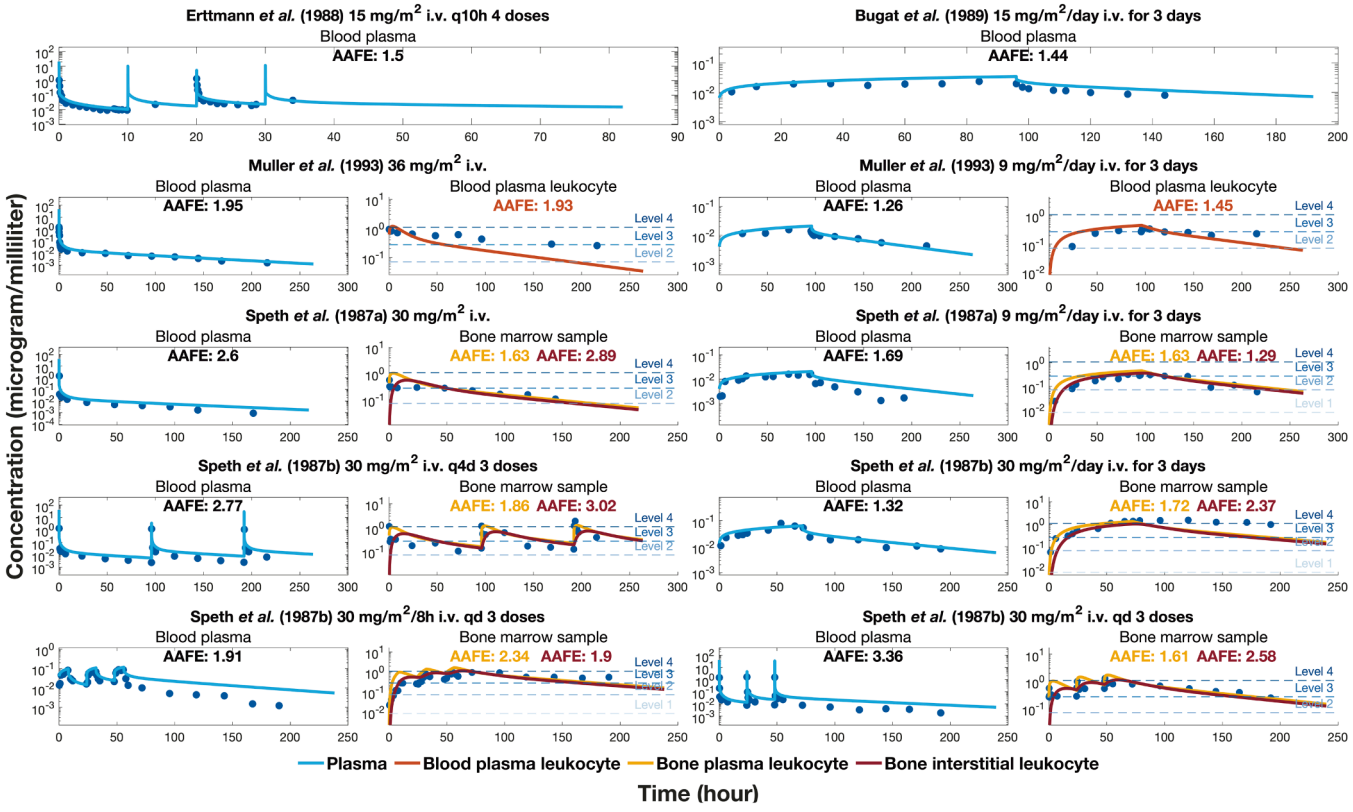

Fig. 3. Comparison of model simulations with clinical data for different dosing schedules in humans. Each simulation corresponds to a specific publication and dosing regimen, as indicated in the title for each subplot. For datasets involving blood mononuclear cells or bone marrow samples, a subplot with the doxorubicin concentration in leukocytes in blood or interstitial and plasma leukocytes in bone was included. The observed data are represented by blue dots, while the light blue line indicates the plasma simulation. The orange line corresponds to the simulation of doxorubicin in blood plasma leukocytes, while the yellow and red lines represent bone plasma and interstitial leukocytes, respectively. The mean absolute fold error (AAFE) for each simulation is calculated and color-coded as previously mentioned. The horizontal dashed lines with different shades of blue indicate the doxorubicin toxicity levels.

concentration for multiple dosing schedules in human clinical data. The mean AAFE for the concentration-time curve was 1.98, with a range of 1.26–3.36 across all datasets. The majority of simulations (seven out of ten) had an AAFE below 2, and only two simulations exceeded an AAFE of 3 (Fig. 3). Moreover, the model demonstrated exceptional predictive performance in estimating doxorubicin concentration at the cellular scale, specifically in leukocytes from both blood and bone. The simulations for doxorubicin in blood leukocytes yielded AAFE values of 1.93 and 1.45 for two datasets. The simulations for peripheral blood admixture in the bone marrow resulted in a mean AAFE of 1.8, with a range of 1.61–2.34 for bone plasma leukocytes and a mean AAFE of 2.34, with a range of 1.29–3.02 for bone interstitial leukocytes. The mixed effect of bone plasma and interstitial leukocytes likely contributed to the observed data's concentration in the bone marrow sample, as suggested by the simulation results. Additionally, the intracellular doxorubicin concentrations fell within the range of level 2–4 toxicity levels, as defined by comparison with the observed data and simulations.

The simulation was conducted using a frequently used clinical dosing schedule of 75 mg/m^2 doxorubicin i.v. at 21-day intervals (Fig. 4). The results showed that doxorubicin concentration was highest in the interstitial space of most organs, which was around 10 times higher than in cellular space and 100 times higher than in plasma. The overall organ concentration was only slightly higher than the cellular concentration. The simulation allowed us to categorize organs into those with low and high accumulation of doxorubicin in cellular space. Organ such as muscle, skin, adipose, bone, lung, lymph node, and brain had low cellular doxorubicin accumulation, whereas the heart, kidney, gonads, and organs in the digestive system had higher cellular doxorubicin accumulation. Additionally, after 21 days, cellular concentrations of doxorubicin in every organ could potentially reach or decrease to a level of 1 toxicity or lower.

The results from Fig. 5A indicated that multiple dosing regimens resulted in toxicity levels for various cell types. Specifically, blood plasma and skin cell toxicity levels were considered level 1, adipose cell toxicity was level 2, bone cell toxicity was level 3, blood plasma leukocyte, bone plasma and interstitial leukocyte, and stomach cell toxicity were level 4. These levels were determined based on reported toxic dosing regimens, and all three simulations yielded similar results. To calculate the AUC values for the cells, we used reported toxicity dosing schedules and maximum lifetime cumulative dose of 75 mg/m^2 i.v. q3w 8 doses simulations, as shown in Fig. 5A and Fig. 5C, respectively. The four simulations generated similar AUC values. For instance, the mean AUC_{L4} for all leukocyte sub-compartments was 129.68 μg/mL*h (range: 34.67–280.18). In contrast, the mean AUC_{L4} for cell sub-compartments in the heart and stomach was 177.91 and 219.1 μg/mL*h (range: 92.85–286.55 and 114.92–346.97), respectively. The mean AUC_{L3} for bone cell was 6.73 μg/mL*h (range: 0–21.82). However, skin and adipose cells had low doxorubicin accumulation, resulting in AUC_{L1} and AUC_{L2} values below 10 μg/mL*h, with some simulations resulting in 0 μg/mL*h.

Comparing these findings with Fig. 5B, we can confirm the defined toxicity levels for these cells. The drug concentration did not exceed or only slightly exceeded these levels, validating our previous conclusions.

4. Discussion

The application of PBPK models in clinical settings has traditionally been limited to predicting drug concentrations in plasma, without

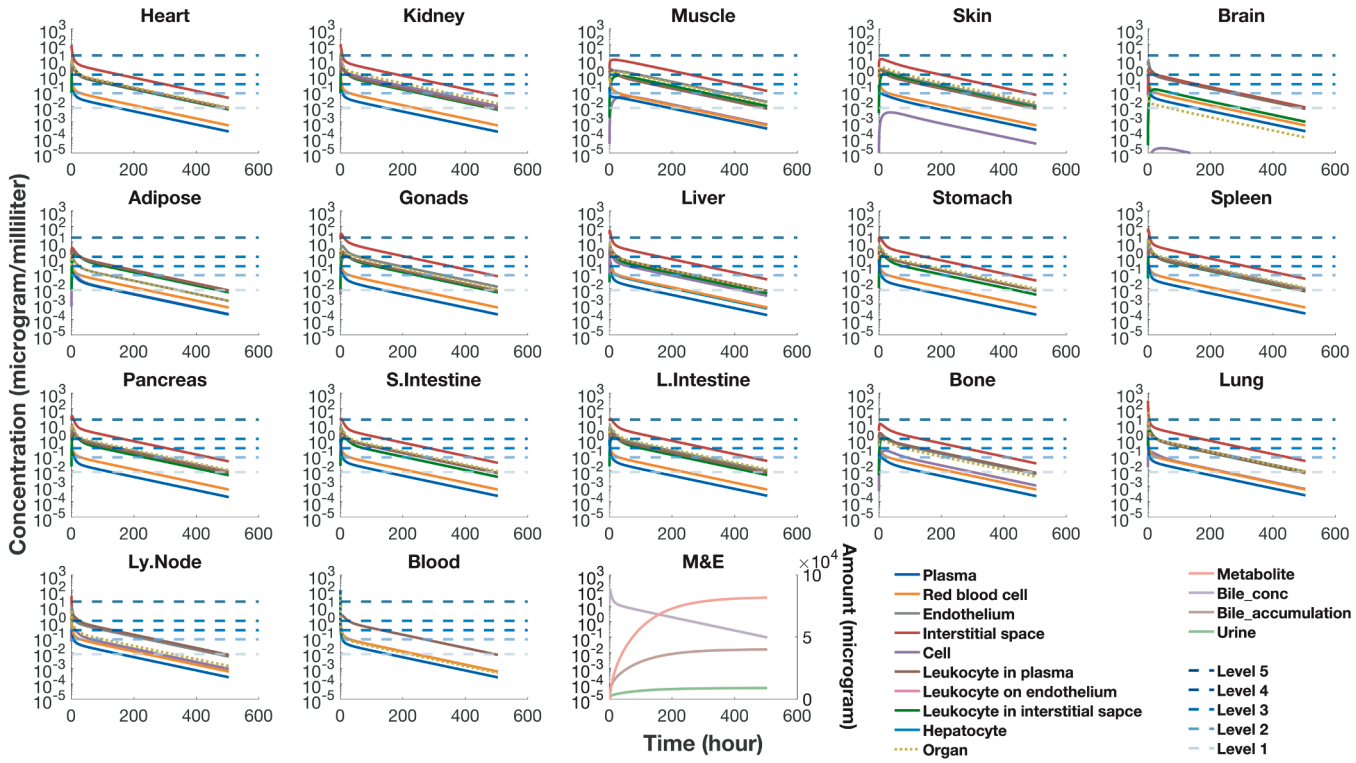
Heart
Kidney
Muscle
Skin
Brain
Adipose
Gonads
Liver
Stomach
Spleen
Pancreas
S.Intestine
L.Intestine
Bone
Lung
Ly.Node
Blood
M&E
Concentration (microgram/milliliter)
Amount (microgram)
Time (hour)
Plasma
Red blood cell
Endothelium
Interstitial space
Cell
Leukocyte in plasma
Leukocyte on endothelium
Leukocyte in interstitial sapce
Hepatocyte
Organ
Metabolite
Bile_conc
Bile_accumulation
Urine
Level 5
Level 4
Level 3
Level 2
Level 1 considering organ or sub-organ scale concentrations. However, the complexity of PBPK models and the large number of parameters and compartments involved can lead to overparameterization, limiting the full potential of this approach [7]. In this study, we developed and validated a PBPK model for doxorubicin that considers realistic physiology and anatomy through interspecies extrapolation and multiple datasets. Our model accurately predicted doxorubicin disposition in vivo, including multiple (sub-)compartments, elimination, and metabolism behavior as well as clinical PK studies on both plasma and cellular scales. We also used our model to quantitatively assess the potential clinical toxicity of doxorubicin at a cellular level. To our knowledge, our doxorubicin PBPK model is the first to incorporate extensive evaluations of doxorubicin concentration in preclinical and clinical datasets, providing a novel approach for toxicity assessment in clinical practice.

In order to avoid the overfitting of the model, we imposed a constraint on the number of estimated parameters to six, which were applied uniformly across multiple organs. In contrast, typical PBPK models for doxorubicin reply on over ten parameters and heavily depend on organ-specific permeability surface area product or tissue partition coefficient to achieve adequate fitting [29,30]. Our model also incorporates the consideration of nonspecific binding in the interstitial space, which provides a novel perspective on the potential disposition of doxorubicin in vivo. Conventionally, PBPK model assume that the interstitial space contains only fluid, while published models for doxorubicin introduced an additional intracellular binding site to account for doxorubicin's binding to DNA and cardiolipin. However, this approach may result in an excessively high concentration of doxorubicin in the additional intracellular binding site [30,31] which could cause severe toxicity or DNA damage [32–35]. As an alternative, we propose considering the nonspecific binding of doxorubicin in the extracellular matrix (ECM) of the interstitial space to explain its prolonged tissue retention, which is supported by histological studies of doxorubicin in tissue [36–38]. Our estimated value of P_{para} of 0.02 cm/min, compared to the calculated permeability of the doxorubicin through cell member of 2.98×10^{-5} cm/min, is consistent with other published works [39,40]. This finding implies that the transport of the doxorubicin through the endothelium is not solely due to diffusion, but convection also play a role [41].

The overall AAFE for model prediction in humans was found to be 2.12 as depicted in Fig. 1. However, doxorubicin pharmacokinetics often exhibit substantial inter-individual variability, which can be several folds different within a single study [6,42]. Furthermore, the dataset used in this study was collected from multiple publications, thereby introducing additional uncertainty in the results. Despite these challenges, the model's performance was considered adequate. However, the published data typically had unequal study durations and unclear inter-individual variation evaluations, which limited the development of a more detailed individual-oriented model that considers the uncertainty.

Fig. 3 presents the experimental cellular data and simulations that not only confirmed the model's prediction performance on a cellular scale but also supported with the defined toxicity level. The clinical data with cellular concentration obtained from Muller et al. (1993) included patients with chronic lymphocytic leukemia, Speth et al. (1987a) included patients with multiple myeloma, and Speth et al. (1987b) included patients with acute nonlymphocytic leukemia, chronic myeloid leukemia, and end-stage Hodgkin's disease. The data and simulations fell between level 2–4 toxicity levels, defined as the median of GI50, the median of IC50 and the 75th percentile of IC50 during the study period.

A quantitative assessment of doxorubicin toxicity levels was performed to support the clinically used dosing schedule of 75 mg/m2 i.v.

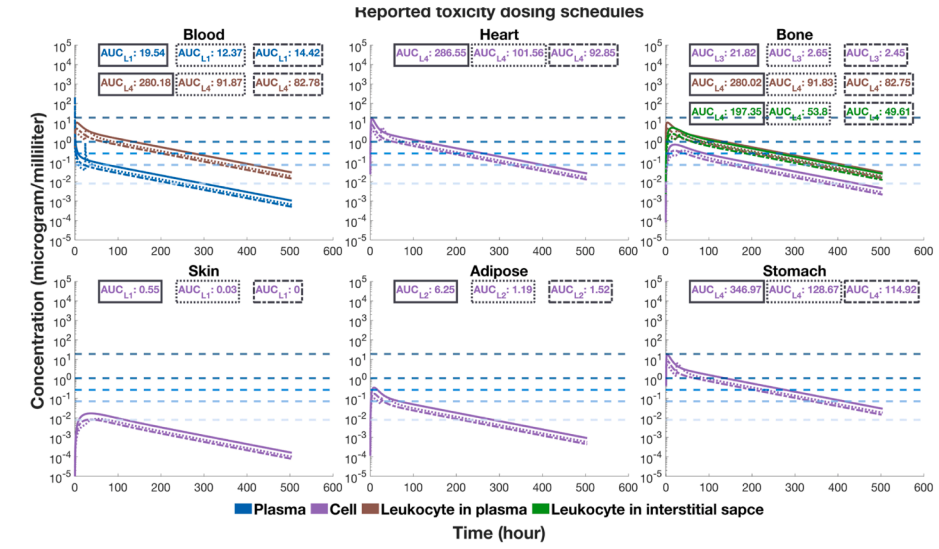

B

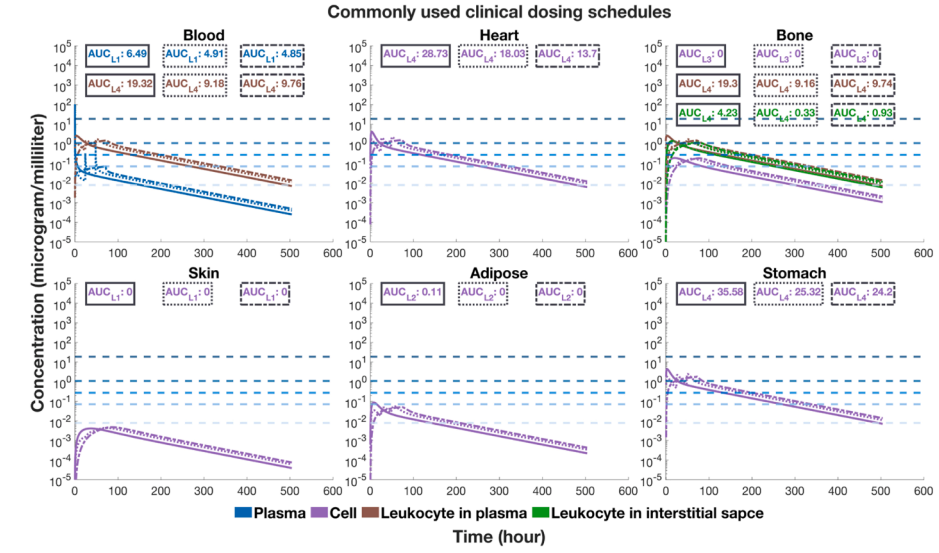

C

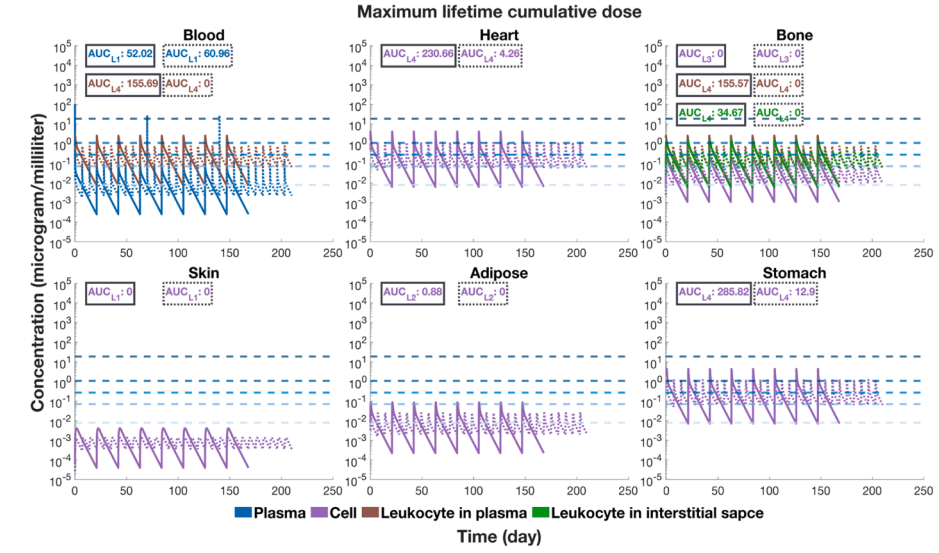

(caption on next page)

Fig. 5. Simulations of doxorubicin clinical toxicity assessments. (A) Three different dosing regimens of doxorubicin were simulated using the two reported accidental overdose cases of doxorubicin from Bäck et al. (1995) [27] with dosing regimen of 540 mg i.v. with 0.75 h infusion (solid line) and 150 mg i.v. qd 2 doses (dot line) and 150 mg/m^2 i.v. (dot-dash line) considered as fatal dose [5] from Micromedex® Drug Reference simulations (B) The simulation of commonly used clinical dosing regimens [1] of 75 mg/m^2 (solid line), 30 mg/m^2 i.v. qd 3 doses (dot line), and 100 mg/m^2 i.v. 72 h infusion (dot-dash line) simulations (C) The maximum lifetime cumulative dose of doxorubicin was simulated using a dosing regimen of 75 mg/m^2 i.v. q3w 8 doses (solid line) and a dosing regimen proposed by Weiss & Manthel (1977) [28] of 20 mg/m^2 i.v. qw 30 doses (dot line). The sub-compartments and organs simulated, including blood, heart, bone, skin, adipose, and stomach, were color-coded and labeled at the bottom of each subfigure. The area under curve (AUC) values, including AUC_{L1}, AUC_{L2}, AUC_{L3}, and AUC_{L4}, were calculated above toxicity levels 1, 2, 3, and 4, respectively, with a unit of μg/mL*h. The predefined toxicity levels were represented by horizontal dash lines with different shades of blue. The AUC values were labeled based on the above-mentioned line style and text color in the legend.

administered at 21-day intervals. Based on the simulation in Fig. 4, the cellular concentration of doxorubicin could decrease below the level 1 toxicity (5th percentile of IC50) indicating that there is barely any toxicity effect from doxorubicin in the cell at this level. This simulation also suggested that different organs had different affinities to doxorubicin. Among all the studied targets in Fig. 5, skin showed the lowest responsive concentration level. However, in doxorubicin chemotherapy, alopecia had a quite high occurrence rate of 92% [5]. This is likely due to the fact that doxorubicin inhibits cell proliferation or killing the cells through cell cycle arrest at the G(2)/M phase [43], which significantly affects rapidly dividing cells such as skin, but also affects the cells in the gastrointestinal tract and blood cells in the bone marrow, which are commonly reported with AEs. Regarding the two cases of doxorubicin overdosing reported in Bäck et al. (1995) [27], we observed that hematologic toxicity and mucositis occurred, which our defined toxicity level could explain from a cellular perspective. However, in the case of the patient who received a dose regimen of 540 mg i.v. with 0.75 h infusion, acute neurological symptoms appeared, and CNS leukemia developed two months later without any previous clinical or laboratory signs Unfortunately, our model was unable to predict or explain these intermediate to long-term toxicities.

After assessing commonly used clinical dosing schedules, our study supported the use of either separating a single bolus dose into multiple smaller doses or using a slow infusion to reduce the potential development of adverse events. Our evaluation of the cardiotoxicity of doxorubicin provides cellular-scale insight into the findings from Weiss & Manthel (1977) [28] who suggested that the lifetime cumulative dose could be higher when administering doxorubicin 20 mg/m^2 i.v. qw [28], since this dosing regimen could never touch the level 4 toxicity. Our simulation also suggested that the prolongated infusion has advantages that could lower the cytotoxicity of doxorubicin from a cellular perspective, which was aligned with clinical findings [44–47].

Our model and simulation were based on the toxicity associated with the AEs, and did not explore the pharmacodynamics of anti-cancer effect. The anti-cancer effect of doxorubicin is presumed to be dose-dependent [5], and therefore, the physician may prefer single i.v. bolus dosing schedules over others to reach higher cellular concentrations. However, the sensitivity of cancer cells to doxorubicin should always be considered since they are highly divided cells. Hence, by applying tumor compartments and additional information associated with the target cancer type, this model could be used as a good predictor and evaluation tool for decision-making and precision dosing, balancing the benefit and risk.

In conclusion, we have successfully developed a predictive PBPK model for doxorubicin based on interspecies data and interspecies extrapolation simulations, which can predict doxorubicin disposition on multiple tissue levels. This model has the capability to predict doxorubicin disposition in various tissues, making it a valuable tool for both clinical and preclinical in silico studies. We believe that our model has provided unique insights into model construction and quantitative clinical toxicity assessments. However, we acknowledge that the accuracy and precision of our model may be further improved. The data collected from various studies have unequal durations and unclear evaluations of inter-individual variations. Therefore, the development of a more detailed individual-oriented model could improve the accuracy of our predictions. Our model has the potential to guide clinical doxorubicin chemotherapy by providing quantitative toxicity assessments. Furthermore, it can be explored for use in anti-cancer pharmacodynamic (PD) modeling and in vivo disposition outcome evaluations of novel doxorubicin formulations.

Funding

This research was supported by Ministry of Science and Technology, Taiwan (MOST 109–2221-E-038–001-MY3) and National Science and Technology Council, Taiwan (NSTC112–2221-E-038–014). In addition, Fang-Ching Chao is the recipient of the Taiwan Paris-Saclay Doctoral Scholarships between Ministry of Education (Taiwan) and Université Paris-Saclay.

CRediT authorship contribution statement

Fang-Ching Chao: Conceptualization, Data curation, Formal analysis, Investigation, Methodology, Resources, Software, Validation, Visualization, Writing – original draft, Writing – review & editing. **Eloísa Berbel Manaia:** Conceptualization, Methodology, Project administration, Supervision, Validation. **Gilles Ponchel:** Conceptualization, Methodology, Project administration, Supervision, Validation. **Chien-Ming Hsieh:** Formal analysis, Funding acquisition, Investigation, Methodology, Supervision, Writing – review & editing.

Declaration of Competing Interest

There are none.

Data availability

Data will be made available on request.

Acknowledgements

I would like to thank Dr. Morgan Chabanon from CentraleSupélec, Université Paris-Saclay for engaging in discussions and validating the logical consistency of the equations used in the PBPK model.

Appendix A. Supporting information

Supplementary data associated with this article can be found in the online version at doi:10.1016/j.biopha.2023.115636.

References

[1] Doxorubicin hydrochloride injection [highlights of prescribing information]. (Pfizer Inc., New York, NY, 1974) <https://www.accessdata.fda.gov/drugsatfda_docs/label/2013/050467s073lbl.pdf> (Revised October 2013). Accessed January 5, 2023.
[2] Doxil [highlights of prescribing information]. (Alza Corporation, Palo Alto, CA, 1995). <https://www.accessdata.fda.gov/drugsatfda_docs/label/2007/050718s029lbl.pdf> (1995). Accessed December 12, 2022.
[3] S.M. Rafiyath, M. Rasul, B. Lee, G. Wei, G. Lamba, D. Liu, Comparison of safety and toxicity of liposomal doxorubicin vs. conventional anthracyclines: a meta-analysis, Exp. Hematol. Oncol. 1 (2012) 10, https://doi.org/10.1186/2162-3619-1-10.
[4] R. Danesi, S. Fogli, A. Gennari, P. Conte, M. Del Tacca, Pharmacokinetic-pharmacodynamic relationships of the anthracycline anticancer drugs, Clin.

Pharm. 41 (2002) 431–444, https://doi.org/10.2165/00003088-200241060-00004.
[5] Merative Micromedex Drug Reference. Doxrubicin Hydrochloride. <http://www.micromedexsolutions.com> (2023). Accessed January 5, 2023.
[6] S. Eksborg, H.S. Strandler, F. Edsmyr, I. Näslund, P. Tahvanainen, Pharmacokinetic study of IV infusions of adriamycin, Eur. J. Clin. Pharmacol. 28 (1985) 205–212, https://doi.org/10.1007/BF00609693.
[7] J.E. Sager, J. Yu, I. Ragueneau-Majlessi, N. Isoherranen, Physiologically Based Pharmacokinetic (PBPK) modeling and simulation approaches: a systematic review of published models, applications, and model verification, Drug Metab. Dispos. 43 (2015) 1823–1837, https://doi.org/10.1124/dmd.115.065920.
[8] U.S. Food and Drug Administration. Guidance for industry: physiologically based pharmacokinetic analyses —format and content <https://www.fda.gov/downloads/Drugs/ Guida nceCo mplia nceRe gulat oryIn forma tion/Guida nces/UCM531207.pdf> (2018). Accessed January 17, 2022.
[9] H.M. Jones, K. Rowland-Yeo, Basic concepts in physiologically based pharmacokinetic modeling in drug discovery and development, CPT: Pharmacomet. Syst. Pharmacol. 2 (2013) 1–12, https://doi.org/10.1038/psp.2013.41.
[10] I. Nestorov, Whole body pharmacokinetic models, Clin. Pharm. 42 (2003) 883–908, https://doi.org/10.2165/00003088-200342100-00002.
[11] F.Y. Bois, M. Jamei, H.J. Clewell, PBPK modelling of inter-individual variability in the pharmacokinetics of environmental chemicals, Toxicology 278 (2010) 256–267, https://doi.org/10.1016/j.tox.2010.06.007.
[12] H.W. Leung, Development and utilization of physiologically based pharmacokinetic models for toxicological applications, J. Toxicol. Environ. Health 32 (1991) 247–267, https://doi.org/10.1080/15287399109531480.
[13] S. Asami, D. Kiga, A. Konagaya, Constraint-based perturbation analysis with cluster Newton method: a case study of personalized parameter estimations with irinotecan whole-body physiologically based pharmacokinetic model, BMC Syst. Biol. 11 (2017) 129, https://doi.org/10.1186/s12918-017-0513-2.
[14] Y. Yang, Y. Chen, L. Wang, S. Xu, G. Fang, X. Guo, Z. Chen, Z. Gu, PBPK modeling on organs-on-chips: an overview of recent advancements, Front Bioeng. Biotechnol. 10 (2022), 900481, https://doi.org/10.3389/fbioe.2022.900481.
[15] S. Willmann, J. Lippert, M. Sevestre, J. Solodenko, F. Fois, W. Schmitt, PK-Sim®: a physiologically based pharmacokinetic 'whole-body'model, Biosilico 1 (2003) 121–124.
[16] Open Systems Pharmacology., OSP platform on GitHub., <https://github.com/Open-Systems-Pharmacology>. Accessed January 12, 2023.
[17] U. Carlander, D. Li, O. Jolliet, C. Emond, G. Johanson, Toward a general physiologically-based pharmacokinetic model for intravenously injected nanoparticles, Int. J. Nanomed. 11 (2016) 625, https://doi.org/10.2147/IJN.S94370.
[18] Z. Lin, N.A. Monteiro-Riviere, J.E. Riviere, A physiologically based pharmacokinetic model for polyethylene glycol-coated gold nanoparticles of different sizes in adult mice, Nanotoxicology 10 (2016) 162–172, https://doi.org/10.3109/17435390.2015.1027314.
[19] M. Aborig, P.R.V. Malik, S. Nambiar, P. Chelle, J. Darko, A. Mutsaers, A. N. Edginton, A. Fleck, E. Osei, S. Wettig, Biodistribution and physiologically-based pharmacokinetic modeling of gold nanoparticles in mice with interspecies extrapolation, Pharmaceutics 11 (2019) 179, https://doi.org/10.3390/pharmaceutics11040179.
[20] D.J. Griswold, V.D. Champagne, Evaluation of the Coulter S-Plus IV® three-part differential in an acute care hospital, Am. J. Clin. Pathol. 84 (1985) 49–57, https://doi.org/10.1093/ajcp/84.1.49.
[21] R.S. Holdrinet, J. von Egmond, J.M. Wessels, C. Haanen, A method for quantification of peripheral blood admixture in bone marrow aspirates, Exp. Hematol. 8 (1980) 103–107.
[22] R. Erttmann, N. Erb, A. Steinhoff, G. Landbeck, Pharmacokinetics of doxorubicin in man: dose and schedule dependence, J. Cancer Res Clin. Oncol. 114 (1988) 509–513, https://doi.org/10.1007/BF00391502.
[23] R. Bugat, J. Robert, A. Herrera, M.C. Pinel, S. Huet, C. Chevreau, G. Boussin, J. Roquain, M. Carton, Clinical and pharmacokinetic study of 96-h infusions of doxorubicin in advanced cancer patients, Eur. J. Cancer Clin. Oncol. 25 (1989) 505–511, https://doi.org/10.1016/0277-5379(89)90264-2.
[24] C. Muller, E. Chatelut, V. Gualano, M. De Forni, F. Huguet, M. Attal, P. Canal, G. Laurent, Cellular pharmacokinetics of doxorubicin in patients with chronic lymphocytic leukemia: comparison of bolus administration and continuous infusion, Cancer Chemother. Pharm. 32 (1993) 379–384, https://doi.org/10.1007/BF00735923.
[25] P.A.J. Speth, P.C.M. Linssen, R.S.G. Holdrinet, C. Haanen, Plasma and cellular Adriamycin concentrations in patients with myeloma treated with ninety-six-hour continuous infusion, Clin. Pharmacol. Ther. 41 (1987) 661–665, https://doi.org/10.1038/clpt.1987.92.
[26] P.A.J. Speth, P.C.M. Linssen, J.B.M. Boezeman, H.M.C. Wessels, C. Haanen, Cellular and plasma adriamycin concentrations in long-term infusion therapy of leukemia patients, Cancer Chemother. Pharmacol. 20 (1987) 305–310, https://doi.org/10.1007/BF00262581.
[27] H. Bäck, A. Gustavsson, S. Eksborg, S. Rödjer, Accidental doxorubicin overdosage, Acta Oncol. 34 (1995) 533–536, https://doi.org/10.3109/02841869509094021.
[28] A.J. Weiss, R.W. Manthel, Experience with the use of adriamycin in combination with other anticancer agents using a weekly schedule, with particular reference to lack of cardiac toxicity, Cancer 40 (1977) 2046–2052, https://doi.org/10.1002/1097-0142(197711)40:5<2046::aid-cncr2820400508>3.0.co;2-5.
[29] H.P. Chang, Y.K. Cheung, D.K. Shah, Whole-body pharmacokinetics and physiologically based pharmacokinetic model for monomethyl Auristatin E (MMAE, J. Clin. Med. 10 (2021) 1332, https://doi.org/10.3390/jcm10061332.
[30] H. He, C. Liu, Y. Wu, X. Zhang, J. Fan, Y. Cao, A multiscale physiologically-based pharmacokinetic model for doxorubicin to explore its mechanisms of cytotoxicity and cardiotoxicity in human physiological contexts supplementary materials, Pharm. Res. 35 (2018) 174, https://doi.org/10.1007/s11095-018-2456-8.
[31] I.R. Dubbelboer, E. Lilienberg, E. Sjögren, H. Lennernäs, A model-based approach to assessing the importance of intracellular binding sites in doxorubicin disposition supplementary data, Mol. Pharm. 14 (2017) 686–698, https://doi.org/10.1021/acs.molpharmaceut.6b00974.
[32] F. Yang, C.J. Kemp, S. Henikoff, Doxorubicin enhances nucleosome turnover around promoters, Curr. Biol. 23 (2013) 782–787, https://doi.org/10.1016/j.cub.2013.03.043.
[33] D. Gewirtz, A critical evaluation of the mechanisms of action proposed for the antitumor effects of the anthracycline antibiotics adriamycin and daunorubicin, Biochem. Pharmacol. 57 (1999) 727–741, https://doi.org/10.1016/S0006-2952(98)00307-4.
[34] L. Pfitzer, C. Moser, F. Gegenfurtner, A. Arner, F. Foerster, C. Atzberger, T. Zisis, R. Kubisch-Dohmen, J. Busse, R. Smith, G. Timinszky, O.V. Kalinina, R. Müller, E. Wagner, A.M. Vollmar, S. Zahler, Targeting actin inhibits repair of doxorubicin-induced DNA damage: a novel therapeutic approach for combination therapy, Cell Death Dis. 10 (2019) 1–14, https://doi.org/10.1038/s41419-019-1546-9.
[35] V.A. Halim, I. García-Santisteban, D.O. Warmerdam, B. van den Broek, A.J. R. Heck, S. Mohammed, R.H. Medema, Doxorubicin-induced DNA damage causes extensive ubiquitination of ribosomal proteins associated with a decrease in protein translation*, Mol. Cell. Proteom. 17 (2018) 2297–2308, https://doi.org/10.1074/mcp.RA118.000652.
[36] M.R. Dreher, K.V. Sharma, D.L. Woods, G. Reddy, Y. Tang, W.F. Pritchard, O. A. Chiesa, J.W. Karanian, J.A. Esparza, D. Donahue, E.B. Levy, S.L. Willis, A. L. Lewis, B.J. Wood, Radiopaque drug-eluting beads for transcatheter embolotherapy: experimental study of drug penetration and coverage in swine, e4, J. Vasc. Interv. Radiol. 23 (2012) 257–264, https://doi.org/10.1016/j.jvir.2011.10.019.
[37] L. Böckelmann, C. Starzonek, A.-C. Niehoff, U. Karst, J. Thomale, H. Schlüter, C. Bokemeyer, A. Aigner, U. Schumacher, Detection of doxorubicin, cisplatin and therapeutic antibodies in formalin-fixed paraffin-embedded human cancer cells, Histochem Cell Biol. 153 (2020) 367–377, https://doi.org/10.1007/s00418-020-01857-x.
[38] M.G. Wientjes, J.H. Zheng, L. Hu, Y. Gan, J.L.-S. Au, Intraprostatic chemotherapy: distribution and transport mechanisms, Clin. Cancer Res. 11 (2005) 4204–4211, https://doi.org/10.1158/1078-0432.CCR-04-1969.
[39] H.H. Usansky, P.J. Sinko, Estimating human drug oral absorption kinetics from Caco-2 permeability using an absorption-disposition model: model development and evaluation and derivation of analytical solutions for k(a) and F(a), J Pharmacol Exp Ther. 314 (2005) 391–399. https://doi.org/10.1124/jpet.104.076182.
[40] S. Eikenberry, A tumor cord model for Doxorubicin delivery and dose optimization in solid tumors, Theor. Biol. Med Model 6 (2009) 16, https://doi.org/10.1186/1742-4682-6-16.
[41] M.W. Dewhirst, T.W. Secomb, Transport of drugs from blood vessels to tumour tissue, Nat. Rev. Cancer 17 (2017) 738–750, https://doi.org/10.1038/nrc.2017.93.
[42] J.-M. Jacquet, F. Bressolle, M. Galtier, M. Bourrier, D. Donadio, J. Jourdan, J.-F. Rossi, Doxorubicin and doxorubicinol: intra-and inter-individual variations of pharmacokinetic parameters, Cancer Chemother. Pharmacol. 27 (1990) 219–225, https://doi.org/10.1007/BF00685716.
[43] H.-S. Kim, Y.-S. Lee, D.-K. Kim, Doxorubicin exerts cytotoxic effects through cell cycle arrest and Fas-mediated cell death, Pharmacology 84 (2009) 300–309, https://doi.org/10.1159/000245937.
[44] S.P. Ackland, M.J. Ratain, N.J. Vogelzang, K.E. Choi, M. Ruane, J.A. Sinkule, Pharmacokinetics and pharmacodynamics of long-term continuous-infusion doxorubicin, Clin. Pharmacol. Ther. 45 (1989) 340–347, https://doi.org/10.1038/clpt.1989.39.
[45] S.S. Legha, R.S. Benjamin, B. Mackay, M. Ewer, S. Wallace, M. Valdivieso, S. L. Rasmussen, G.R. Blumenschein, E.J. Freireich, Reduction of doxorubicin cardiotoxicity by prolonged continuous intravenous infusion, Ann. Intern Med 96 (1982) 133–139, https://doi.org/10.7326/0003-4819-96-2-133.
[46] I. Popov, S. Jelić, S. Radulović, D. Radosavljević, Z. Nikolić-Tomašević, Eight-hour infusion versus bolus injection of doxorubicin in the EAP regimen in patients with advanced gastric cancer: a prospective randomised trial, Ann. Oncol. 11 (2000) 343–348, https://doi.org/10.1023/A:1008334913109.
[47] J. Shapira, M. Gotfried, M. Lishner, M. Ravid, Reduced cardiotoxicity of doxorubicin by a 6-hour infusion regimen. A prospective randomized evaluation, Cancer 65 (1990) 870–873, https://doi.org/10.1002/1097-0142(19900215)65:4<870::aid-cncr2820650407>3.0.co;2-d.